JOURNAL OF GEOPHYSICAL RESEARCH, VOL. 104, NO. D24, PAGES 31,217–31,224, DECEMBER 27, 1999

A method for monitoring the temporal variation of surface spectral emissivity: Application to thermal infrared multispectral scanner (TIMS) data in HAPEX-Sahel

Zhao-Liang Li, F. Becker,[1] and M.P. Stoll

Laboratires des Sciences de l'Image, de l'Informatique et de la Télédétection, Illkirch, France

Zhengming Wan

Institute for Computational Earth System Science, University of California, Santa Barbara

Abstract. During the Hydrologic Atmospheric Pilot Experiment (HAPEX)-Sahel experiment in 1992, thermal infrared multispectral scanner (TIMS) data were acquired from aircraft at an altitude of 600 m. The main steps to retrieve the surface relative spectral emissivities E from TIMS data using the emissivity normalization method were recalled. Several TIMS data on September 2 and 4 were processed, and the retrieved E for different types of surfaces showed that E in channels 1-3 (8.2-9.4 μm) are less than E in channels 4-6 (9.6-12.0 μm) for bare soils, whereas for vegetation the E profile is not as flat as it should be. In order to correct for the effect of uncertainties in atmospheric profiles given by radiosonde data and to get the emissivity profile flat for vegetation the temperature and humidity profiles were modified by considering the vegetation to be a gray body. Although E obtained with the modified atmospheric profiles seemed to be improved significantly for each day, E obtained for the same type of surface at two days are still very different, showing that it is difficult to compare E derived from different images with the method proposed. Through the comparison of E derived with radiosonde data and E derived with the modified atmospheric profiles the linear relationship found by *Li et al.* [1999] between E calculated with inaccurate atmospheric profiles and its actual value was confirmed. On the basis of this linear relationship property a method called temporal atmospheric normalization was proposed to correct for the errors caused by the imperfect atmospheric corrections under horizontally invariant atmospheric conditions. This method relates linearly the measurement of relative emissivity made at a time t_2, $E^c(t_2)$, to the measurement $E^c(t_2 \rightarrow t_1)$ that would have been made if the atmospheric condition of time t_2 was that of a reference time t_1. In order to calculate the coefficients of the linear relationship between $E^c(t_2 \rightarrow t_1)$ and $E^c(t_2)$ it is necessary to select in the image some samples whose relative emissivity are known to be time invariant. This method was validated using TIMS data. It may now be used to monitor the temporal variation of surface relative emissivity correcting for possible temporal variation of the atmosphere particularly using Advanced Spaceborn Thermal Emission Reflection Radiometer data.

1. Introduction and Objectives

The thermal infrared (TIR) spectral domain has many applications in remote sensing because it not only gives access to the surface temperature but also provides information on the spectral properties of the Earth's surface that may be particularly useful for geologic purposes. In fact, extraction of surface relative TIR emissivity from space or aircraft measurements has been investigated over nearly three decades [*Vincent and Thomson,* 1972; *Kahle et al.,* 1980]. In order to try to get rid of the land surface temperature in this determination, several methods have been developed since then [*Kahle et al.,* 1980; *Gillespie,* 1985; *Kealy and Gabell,* 1990; *Becker and Li,* 1990; *Watson,* 1992], but all of them need accurate atmospheric corrections, which are still a big challenge and are difficult to handle. The new imaging spectro-radiometer Advanced Spaceborn Thermal Emission Reflection Radiometer (ASTER) [*Kahle et al.,* 1991] to be launched shortly will have five bands in the TIR domain, in addition to bands in the visible and near infrared, allowing for detailed mapping and monitoring surface states. It is thus important to get reliable information over long periods, which means information that is quantitatively consistent at different times. Regarding the extraction of the surface TIR emissivity, it is difficult to compare even the relative emissivities derived from different images since all available methods are sensitive to atmospheric errors [*Li et al.,* 1999]. Using simulations, *Li et al.* [1999] showed that the errors caused by an imperfect atmospheric correction on relative emissivity are linearly related to the real values of the relative emissivity. On the

[1]Also at International Space University, Illkirvh, France.

Copyright 1999 by the American Geophysical Union.

Paper number 1999JD900944
0148-0227/99/1999JD900944$09.00

basis of this property we propose in this paper a method referred to as temporal atmospheric normalization to monitor the temporal variation of surface relative emissivity, correcting for eventual temporal variations of atmospheric conditions, and we apply it to several thermal infrared multispectral scanner (TIMS) [*Palluconi and Meeks,* 1985] images collected during Hydrologic Atmospheric Pilot Experiment (HAPEX)-Sahel experiment in 1992 [*Prince et al.,* 1995]. In section 2 we present the procedure which we used in this paper to retrieve the relative spectral emissivities from TIMS data and show in section 3 the effects of uncertainties on atmosphere parameters on the relative emissivity estimate. Finally, we present and discuss, in section 4, the temporal atmospheric normalization method and show that it makes the monitoring of the temporal variation of surface relative spectral emissivity feasible, correcting for eventual temporal variations of atmospheric conditions.

2. Extraction of Relative Spectral Emissivity From TIMS Data

2.1. Data Collections

The TIMS data used below were acquired during the HAPEX-Sahel experiment on September 2 and 4, 1992. The aircraft flight height is 600 m above the ground. For each of the 2 days, data for three flight lines (flights 2, 3, and 4) have been collected, and from them, three subsets (1.5 km x 0.9 km) have been extracted, which constitute our study zones.

TIMS measures thermal radiance in six spectral channels between 8 and 12 μm. The center positions of these six channels are 8.379, 8.782, 9.178, 9.878, 10.711, and 11.637 μm. The nominal noise equivalent temperature difference (NEΔT) of TIMS is 0.3 K. Further details of this instrument are given by *Palluconi and Meeks* [1985].

The atmospheric pressure, temperature, and relative humidity profiles were measured up to 50 hPa by the French National Center of Meteorological Research (CNRM) in Hamdallay near our study zones (these radiosonde data can be found on the World Wide Web at http://www.ird.fr/hapex). The radiosonde data measured closest to the TIMS data acquisition time have been chosen to perform atmospheric corrections and also to estimate the downwelling atmospheric radiance. Table 1 summarizes the auxiliary data information available to authors.

2.2. Data Calibration

Eight bits coded TIMS data have been transformed to physical quantity -radiance using two blackbodies on board as described by *Palluconi and Meeks* [1985]

$$B_i(T_i) = \frac{B_i(\overline{T_h}) - B_i(\overline{T_c})}{\overline{CN}_h - \overline{CN}_c}\left(CN - \overline{CN}_c\right) + B_i(\overline{T_c}), \quad (1)$$

where $B_i(T_i)$ is the channel radiance corresponding to the count number (CN) measured by channel i, $\overline{T}$ and CN are the mean temperature of blackbody and its corresponding mean count number over the subset zone, respectively. $B_i(\overline{T})$ is the channel radiance corresponding to $\overline{T}$. The subscripts h and c indicate hot and cold blackbodies.

2.3. Relative Spectral Emissivity Extraction

Up to now, there exist in the literature six methods for extracting relative spectral emissivity information from thermal infrared multispectral data; they are the reference channel method [*Kahle et al.,* 1980], emissivity normalization method [*Gillespie,* 1985], emissivity renormalization method [*Stoll,* 1993], temperature-independent spectral indices (TISI) method [*Becker and Li,* 1990], spectral ratio method [*Watson,* 1992], and alpha emissivity method [*Kealy and Gabell,* 1990]. The performance of these six methods has been recently discussed and evaluated by *Gillespie et al.* [1996] (this document can be found on the World Wide Web at http://asterweb.jpl.nasa.gov/asterhome/atbd) and *Li et al.* [1999]. Considering the overall error that may occur in real data, they concluded that the TISI and emissivity normalization methods are slightly superior to other methods. Since the concept of emissivity normalization method is straightforward and simple, we use it in this paper to extract the relative spectral emissivity from the calibrated TIMS data given by (1). The main steps of this method are briefly described below [*Realmuto,* 1990; *Li et al.,* 1999].

First, a constant emissivity ε is assumed in all N channels for a given pixel, which enables N channel surface temperatures T_{si} (i=1, N) to be calculated for each pixel from their measured radiance $B_i(T_i)$ using

$$T_{si} = B_i^{-1}\left[\frac{B_i(T_i) - R_{ati\uparrow} - (1-\varepsilon)R_{ati\downarrow}\tau_i}{\varepsilon\tau_i}\right], \quad (2)$$

where τ_i, $R_{ati\uparrow}$, and $R_{ati\downarrow}$ are the channel atmospheric transmission, the channel upwelling atmospheric radiance, and the channel downwelling hemispheric atmospheric radiance divided by π, respectively.

Then the highest of those N channel surface temperatures T_{si} is considered to represent the land surface temperature T_s and used to derive emissivity values for the other channels from

$$\varepsilon_i = \frac{(B_i(T_i) - R_{ati\uparrow})/\tau_i - R_{ati\downarrow}}{B_i(T_s) - R_{ati\downarrow}} = \frac{B_i(T_{gi}) - R_{ati\downarrow}}{B_i(T_s) - R_{ati\downarrow}}, \quad (3)$$

where $B_i(T_{gi})$ is the channel radiance measured at ground level and T_{gi} is the surface brightness temperature in channel i.

Supposing that the highest of the channel surface temperatures for a given pixel occurs in channel k ($T_{sk} = \max(T_{si})$), which means that the emissivity in channel k, ε_k, is the maximum for this pixel and $\varepsilon = \varepsilon_k$. As demonstrated by *Li et al.* [1999], the derived emissivity value ε_i divided by $\varepsilon_k^{n_{ik}}$ is almost independent of the value of ε_k used in (2). Here the exponent n_{ik} is the ratio of n_i to n_k, and n is the exponent of the power law by which the Planck's function is approximated [*Slater,* 1980].

Moreover, because ε_k and n_{ik} are close to unity for TIMS channels [*Becker and Li,* 1990], denoting E_{ik} as the relative emissivity of channel i to channel k, that is,

$$E_{ik} = \frac{\varepsilon_i}{\varepsilon_k}, \quad (4)$$

we have [*Li et al.,* 1999]

$$E_{ik} \cong \frac{\varepsilon_i}{\varepsilon_k^{n_{ik}}} \cong \frac{B_i(T_{gi}) - R_{ati\downarrow}}{B_i(T_{gk}) - R_{ati\downarrow}}. \quad (5)$$

Table 1. Data Information Summary

Date	TIMS Data			Radiosonde Data			
	Flight Line	Spatial Resolution, m	Acquisition Time, h, min	Acquisition Time, h, min	T_a^*, K	$W^\dagger$ (up to infinity), g/cm^2	$W^\dagger$ (up to 600 m), g/cm^2
Sept. 2 (Day 246)	2	1.5	12, 52	12, 57	304.5	4.32	0.94
	3		13, 18				
	4		13, 37				
Sept. 4 (Day 248)	2	1.5	13, 42	10, 30	304.5	4.18	0.97
	3		14, 01				
	4		14, 17				

$^*T_a$ is the air temperature in the first layer of atmosphere (K).

$^\dagger W$ is the total column water vapor content (g/cm^2).

From the procedures described above ((3) and (5)) we noted that the atmospheric quantities τ_i, $R_{ati}\uparrow$, and $R_{ati}\downarrow$ must be known to apply the method. For our cases they have been estimated by running Modtran 3.5 [*Kneizys et al.*, 1996] with the radiosonde data as its input. Setting arbitrarily the maximum value of emissivity among six channels ε_k to be 0.97, the relative emissivity E_{ik} is extracted by successively applying (2), (3), and (4) or (5) to TIMS data.

To make the interpretation of the relative spectral emissivities for different types of surfaces easier, channel 5 of TIMS was taken for all pixels as the reference channel. From (4) it is simple to get E_{i5} by

$$E_{i5} = \frac{E_{ik}}{E_{5k}} \quad \text{for all } k. \tag{6}$$

As an example, Figures 1a and 2a display the spectral variation of the relative emissivity E_{i5} derived from TIMS data of flight 4 on day 246 and day 248, respectively, for different types of surfaces. The brief descriptions of these different types of surfaces are given in Table 2. Further details of the mineralogical and granulometric compositions of these types of soils can be found in Table 2 of *Houssa et al.* [1996]. Each value shown is the average over 15x15 pixel values on the same type of surface. We note the following observations.

1. For the same type of surface the shape of the relative emissivity curves and their values are very different from one day to another. However, field observations indicate that there was no detectable change in the surface emissivity for these types of surfaces [*Nerry et al.*, 1996] (these field observation can be found on the World Wide Web at http://www.ird.fr/hapex).

2. The relative emissivity curve for vegetation is not as flat as it should be since vegetation spectral emissivity does not change much over the TIR domain, particularly for day 246 where the relative emissivities in channels 1 and 6 are lower than the others.

The same findings are observed for flight lines 2 and 3. We thought this abnormality was caused by the imperfect atmospheric corrections because of uncertainties in atmospheric profiles. Following the method proposed by *Steyn-Ross et al.* [1993, 1997], we modify the temperature and humidity (H) profiles with the vegetation pixels in the following ways: (1) keep the adiabatic rate unchanged and modify the air temperature T_a by adding a constant ΔT_a up to 8 km (modified $T_a(z)$ = measured $T_a(z) + \Delta T_a$ for $z < 8$ km) and (2) modify the humidity H by a scaling factor F (modified $H(z)$ = measured $H(z)*F$).

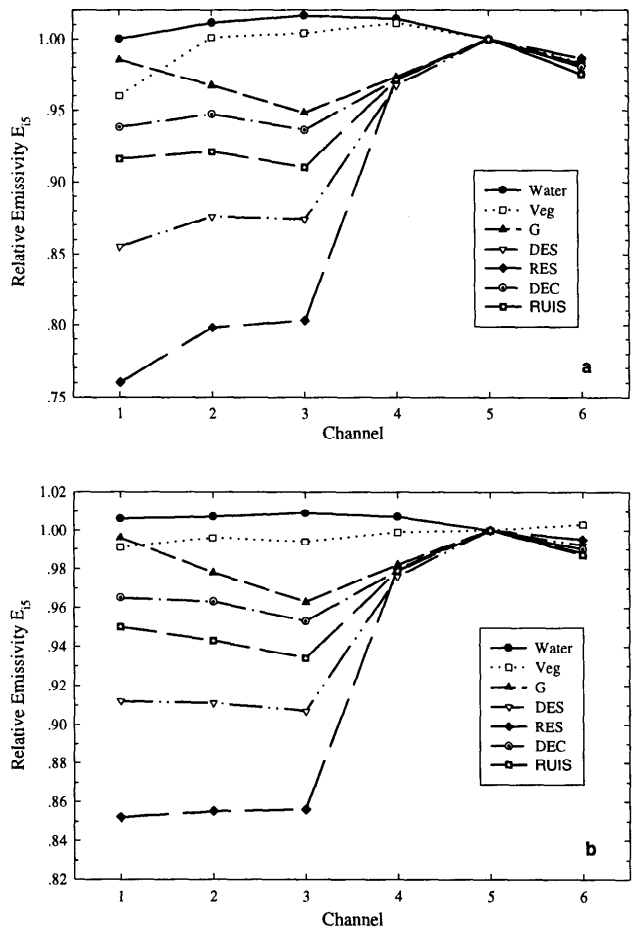

Figure 1. Relative spectral emissivity E_{i5}^c derived from TIMS data (flight line 4, day 246) by the emissivity normalization method for different types of surfaces described in Table 2. The mineralogical and granulometric compositions of these types of soils have been given in Table 2 of *Houssa et al.* [1996]. (a) With radiosonde data and (b) with modified radiosonde data.

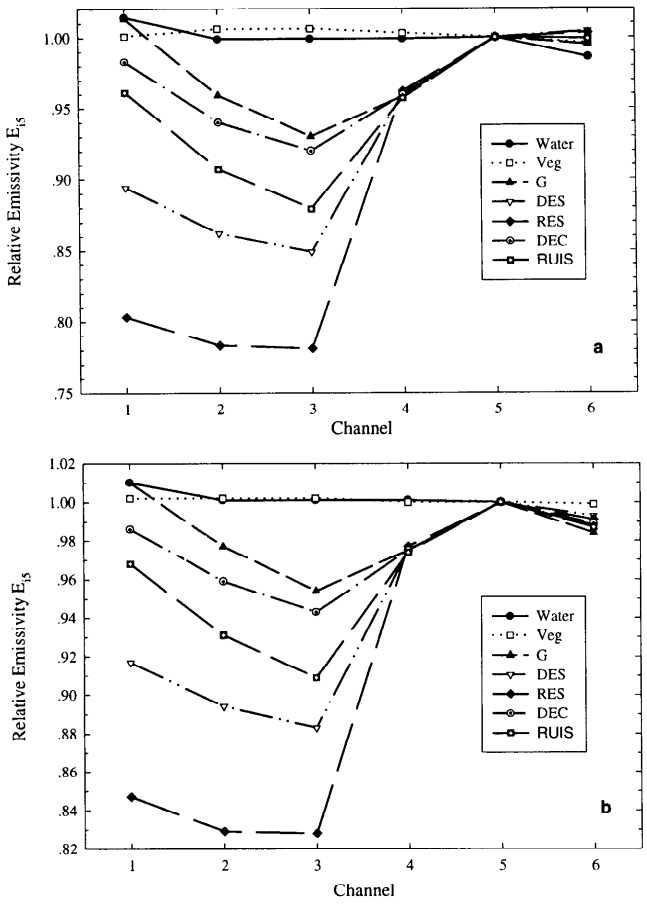

Figure 2. Same as Figure 1 but for flight line 4 of day 248.

Since the aim of these modifications is to get no spectral variation of the emissivity for vegetation pixels, we first selected a box of 20x20 pixels of vegetation near the nadir view and took the average of their brightness temperatures to reduce the instrumental noise, and then, assuming that vegetation is a good gray body, a nonlinear least squares method was used to get four unknowns (surface emissivity, surface temperature, ΔT_a, and F) from six brightness temperatures (six equations, one for each channel of TIMS)[*Wan and Li,* 1997]. The results we got for vegetation surface are shown in Table 3.

It is interesting to note that for a given day the atmospheric parameters adjusted on vegetation pixels given in Table 3 are more or less the same for the different flights. If we assume that the values in Table 3 are plausible, then the air temperature measured by radiosonde should be corrected for by about -3.8 K for day 246 and -1.6 K for day 248, and the water vapor profile (H) is modified by a factor of 0.65-0.79 for both days. The emissivity derived for vegetation varies from 0.964 to 0.974 for day 246 and 0.958 to 0.960 for day 248. Those values are a little bit smaller than the expected values for vegetation.

In order to check the improvement resulting from the modified atmospheric profile, we recomputed the relative emissivity for the above samples with the modified profiles. Figures 1b and 2b display the results corresponding to Figures 1a and 2a, respectively. We note the following observations.

1. The vegetation spectral shape is significantly improved, particularly for day 246, although this sample is not the sample we took to modify the atmospheric profiles.

2. The water spectral signature is not flat because the water is very dirty in the study area (J.C. Pion, University of Strasbourg, personal communication, 1997).

3. For bare soils the relative emissivities in the lower channels (channels 1, 2, and 3) are smaller than those in the higher channels (channels 4, 5, and 6) as observed by *Schmugge et al.* [1991] on HAPEX-Mobilhy region. The large variation of the spectral emissivities in channels 1 and 3 is observed for different types of surfaces; it is therefore useful to introduce two normalization emissivity indices, namely; $(E_{15}-E_{35})/(E_{15}+E_{35})$ and $(E_{35}-E_{45})/(E_{35}+E_{45})$, to discriminate between the different types of surfaces. This will be demonstrated in a future work.

4. For the same type of surface the values of the relative emissivities for two days are still very different. According to the field observations, there were no detectable changes of surface properties between these two days [*Nerry et al.,* 1996]. The difference we observed from TIMS images may therefore be due to the absolute calibration errors of TIMS channels, which very much affect the results of nonlinear least squares method.

In conclusion, even though we modified the atmospheric profiles with vegetation pixel, we are still unable to get reliable information that is quantitatively consistent at different times using the available methods because all methods are sensitive to atmospheric errors. In sections 3 and 4, on the basis of the linear relationship between the actual values of the relative emissivities and those derived with inaccurate atmospheric profiles, we propose a method to make it possible to intercompare different images over the same region.

3. Effects of Atmospheric Uncertainties on Relative Emissivity Retrievals From TIMS Data

By mathematical demonstration and calculations on simulated data, *Li et al.* [1999] showed that the relative

Table 2. Descriptions of Different Types of Surfaces Presented in Figures 1 and 2

Type of Surface	Description
Water	dirty water
Veg	vegetation
G	crust with gravels (>2mm)
DES	crust not cultivated, slightly developed over the eolian sand
RES	red eolian sand
DEC	crust not cultivated, developed over organized surface
RUIS	crust not cultivated, developed over sandy surface

Table 3. Four Parameters (ΔT_a , F, T_s, and ε) Adjusted Using a Nonlinear Least Squares Method for Vegetation Pixels Taken From Different Flight Lines and Different Days

		Day 246			Day 248		
		Flight 2	Flight 3	Flight 4	Flight 2	Flight 3	Flight 4
Atmospheric variables	ΔT_a^*, K	-3.6	-4.0	-3.9	-1.9	-1.0	-2.0
	F^*	0.75	0.65	0.77	0.77	0.79	0.65
Reference surface parameters	$T_s^\dagger$, K	302.3	298.6	298.7	304.5	305.3	305.9
	$\varepsilon^\dagger$	0.974	0.967	0.964	0.958	0.958	0.960

* ΔT_a is the difference of air temperature estimated by the proposed method and that measured by radiosonde; F is the ratio of relative humidity estimated by the proposed method to that measured by radiosonde.
† T_s and ε are surface temperature and emissivity estimated by the proposed method for vegetation, respectively.

emissivity E_{i5}^c derived with inaccurate atmospheric parameters is linearly related to its actual value E_{i5} , namely,

$$E_{i5}^c = a_i E_{i5} + b_i \,, \tag{7}$$

where

$$a_i = \frac{\left(1 - R_{ati\downarrow}/B_i(T_s)\right)\left(1 + n_i\,\Delta T_{gi}/T_{gi}\right)}{1 - R_{ati\downarrow}/B_i(T_s)\left(1 + \Delta R_{ati\downarrow}/R_{ati\downarrow}\right) + n_5\,\Delta T_{g5}/T_{g5}}$$

$$b_i = \frac{-R_{ati\downarrow}/B_i(T_s)\left(\Delta R_{ati\downarrow}/R_{ati\downarrow} - n_i\,\Delta T_{gi}/T_{gi}\right)}{1 - R_{ati\downarrow}/B_i(T_s)\left(1 + \Delta R_{ati\downarrow}/R_{ati\downarrow}\right) + n_5\,\Delta T_{g5}/T_{g5}} \,,$$

where $\Delta R_{ati\downarrow}$, ΔT_{gi} , and ΔT_{g5} are the errors on $R_{ati\downarrow}$, T_{gi} , and T_{g5} that resulted in the inaccuracies of the atmospheric characterizations in the atmospheric corrections. As shown by *Li et al.* [1999], the coefficients a_i and b_i are only weakly dependent of surface temperature T_s , and in the cases where the atmospheric corrections are performed with the radiosonde data or the atmosphere is relatively dry they are only a function of atmospheric parameters and the errors in those parameters.

To check whether the linear relationship between E_{i5}^c and E_{i5} expressed by (7) exists for real data, we calculated the relative emissivity E_{i5}^c from TIMS data using both the radiosonde data and the modified atmospheric profiles (water vapor profile (H) has been modified by a factor of 0.6 and 0.8, and ΔT_a=0). If we assume that E_{i5}^c derived with radiosonde data is the true value of E_{i5} , the linear correlation between the relative emissivities E_{i5} and those derived with the modified profiles should exist as predicted by (7). Figure 3 shows those correlation for channel 1 and for two columns of image (flight 4 of day 246). Those two columns correspond to two view angles, 0° and 30°, respectively. We note that at least for this image, (1) the linear correlation exists and (2) the slope and offset of those linear relations are almost independent of view angle.

Another example is given in Figure 4, in which the correlation between E_{i5}^c (Figures 1a and 2a) calculated with radiosonde data and E_{i5}^c (Figures 1b and 2b) calculated with the modified atmospheric profiles is displayed. As predicated by (7), the linear correlation is observed. In conclusion, the results presented in this section confirm the linear correlation between E_{i5}^c and E_{i5} .

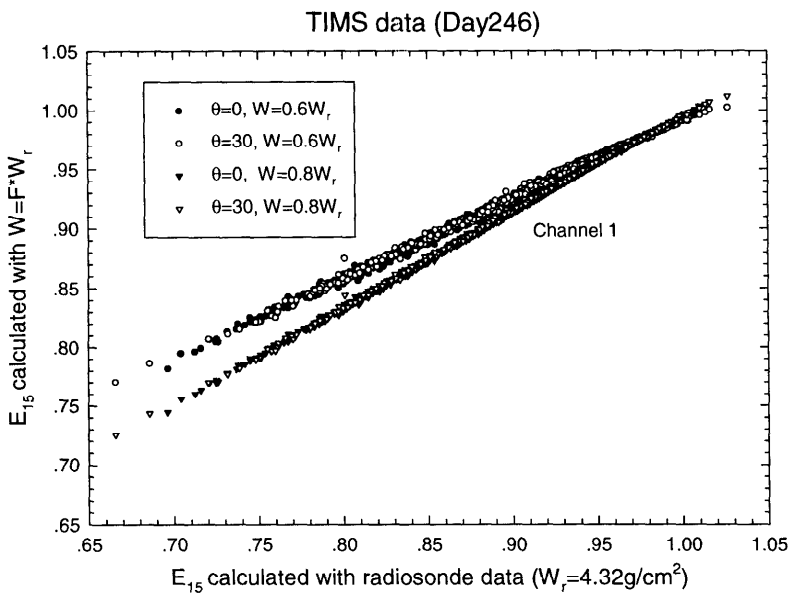

Figure 3. Illustration of the linear relationship between E_{i5}^c derived from TIMS data (day 246) with radiosonde data (water vapor content $W = W_r = 4.32$ g/cm^2) and E_{i5}^c derived with deviate atmospheres (W=$0.6W_r$, and W=$0.8W_r$) for two view angles (nadir and 30°).

4. Temporal Atmospheric Normalization Method

4.1. Principle of Method

As illustrated above, the effects of errors in atmospheric corrections on relative emissivities are linear. On the basis of this property we propose a method called the temporal atmospheric normalization method to monitor the temporal variation of surface relative spectral emissivity, taking into account possible atmospheric variations. This method needs only a chosen reference time, referred to as time t_1, and an assumption that in the image, there are some pixels, denoted as set s, for which no temporal change in relative emissivity occurs from reference time t_1 to another time t_2. In order to simplify the mathematical notations we omit in the following the channel indices i and 5 in (7) and denote E_s as the actual relative emissivity E of the pixel in set s and $E_s^c(t_1)$ and $E_s^c(t_2)$ as the relative emissivity calculated for the pixel within the set s at time t_1 and time t_2 with the corresponding approximate atmospheric parameters, respectively. According to (7), one can write

$$E_s^c(t_1) = a(t_1)E_s + b(t_1)$$

$$E_s^c(t_2) = a(t_2)E_s + b(t_2).$$

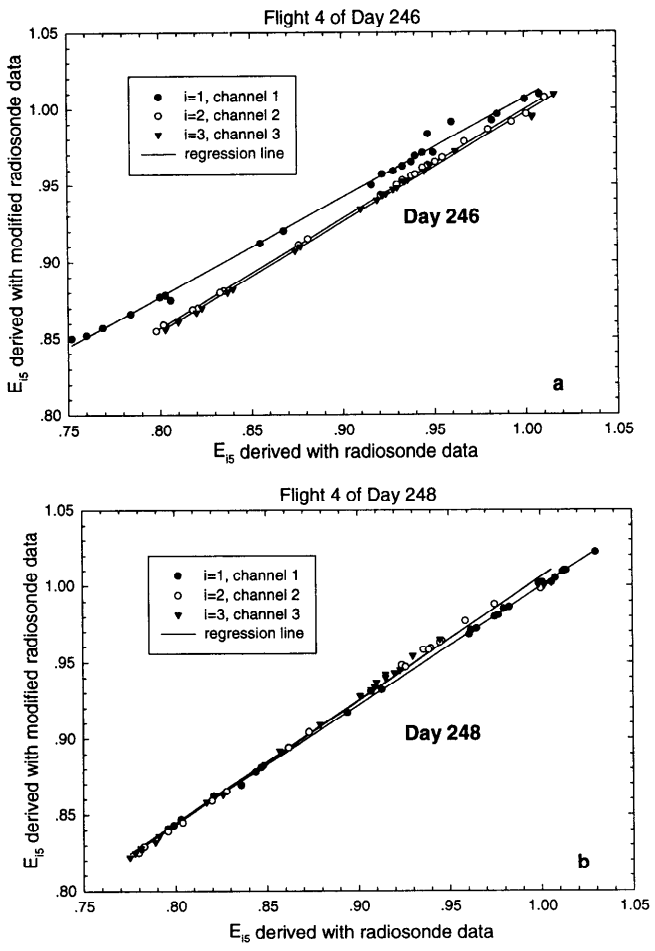

Figure 4. Illustration of the linear relationship between E_{i5}^c derived with radiosonde data (Figures 1a and 2a) and that derived with modified radiosonde data (Figures 1b and 2b) for flight line 4 and channels 1-3 of TIMS (a) for day 246 and (b) for day 248.

Eliminating E_s between these two equations leads to

$$E_s^c(t_2) = a(t_2 \to t_1)E_s^c(t_1) + b(t_2 \to t_1), \tag{8}$$

with

$$a(t_2 \to t_1) = \frac{a(t_2)}{a(t_1)} \quad \text{and} \quad b(t_2 \to t_1) = b(t_2) - a(t_2 \to t_1)b(t_1).$$

Assuming that the effects of spatial variations of the atmospheric conditions within the image at times t_1 and t_2 are not larger than the effect of instrument noise or that the temporal variations of the atmospheric conditions for the whole image are the same, the linear relationship given by (8) holds for any pixel in the image, that is,

$$E^c(t_2) = a(t_2 \to t_1)E^c(t_2 \to t_1) + b(t_2 \to t_1), \tag{9}$$

where $E^c(t_2)$ is the relative emissivity calculated at time t_2 using the emissivity normalization method with the atmospheric parameters of time t_2, and $E^c(t_2 \to t_1)$ is the relative emissivity at time t_2 which would be obtained if the relative emissivity of time t_2 was measured with the atmospheric condition of time t_1.

Therefore it is possible to normalize the relative emissivity measured at time t_2 as if it were measured with the atmospheric conditions of time t_1 by inverting (9), namely,

$$E^c(t_2 \to t_1) = \frac{E^c(t_2) - b(t_2 \to t_1)}{a(t_2 \to t_1)}. \tag{10}$$

This method normalizes the atmospheric condition of time t_2 to that of time t_1, which is why we call it "temporal atmospheric normalization."

It should be noted that for a given pixel the difference between $E^c(t_2)$ and $E^c(t_1)$ accounts for both the difference between the actual relative emissivity $E(t_2)$ and $E(t_1)$ and the difference between the effects of the atmospheric parameters errors at time t_2 and time t_1, while the difference between $E^c(t_2 - t_1)$ and $E^c(t_1)$ accounts only for the difference between the actual relative emissivity $E(t_2)$ and $E(t_1)$. From the principle of the method, if the actual emissivity does not change between time t_1 and t_2, it is obvious that $E^c(t_2 \to t_1) = E^c(t_1)$, as seen by comparing (9) with (8). On the other hand, if $E^c(t_2 \to t_1) \neq E^c(t_1)$, this implies that the actual relative emissivity does change from time t_1 to time t_2. Hence it is possible to monitor the temporal variation of the relative emissivity E^c using the temporal atmospheric normalization method without knowing the exact atmospheric parameters at times t_1 and t_2.

4.2. Validation

The temporal atmospheric normalization method is applied to TIMS data described in section 2.1. First, we calculate the relative emissivities from TIMS data acquired on day 246 (time t_1) and day 248 (time t_2) using the emissivity normalization method with their corresponding radiosonde data. Second, on the basis of a priori knowledge we identify in the images some pixels whose relative emissivities are assumed to be time invariant between days 246 and 248. Third, we take the relative emissivities derived from TIMS data on day 246 as $E^c(t_1)$ and those derived from day 248 as $E^c(t_2)$, and we show, as an example, in Figure 5 the correlation between $E^c(t_1)$ and $E^c(t_2)$ for the pixels

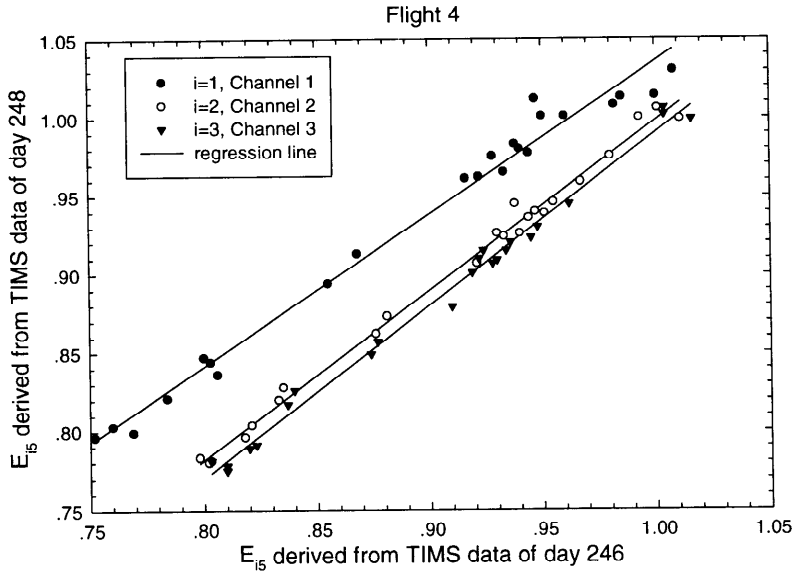

Figure 5. Correlation of E_{i5}^{c} (Figures 1a and 2a) derived from two different days with their corresponding radiosonde data.

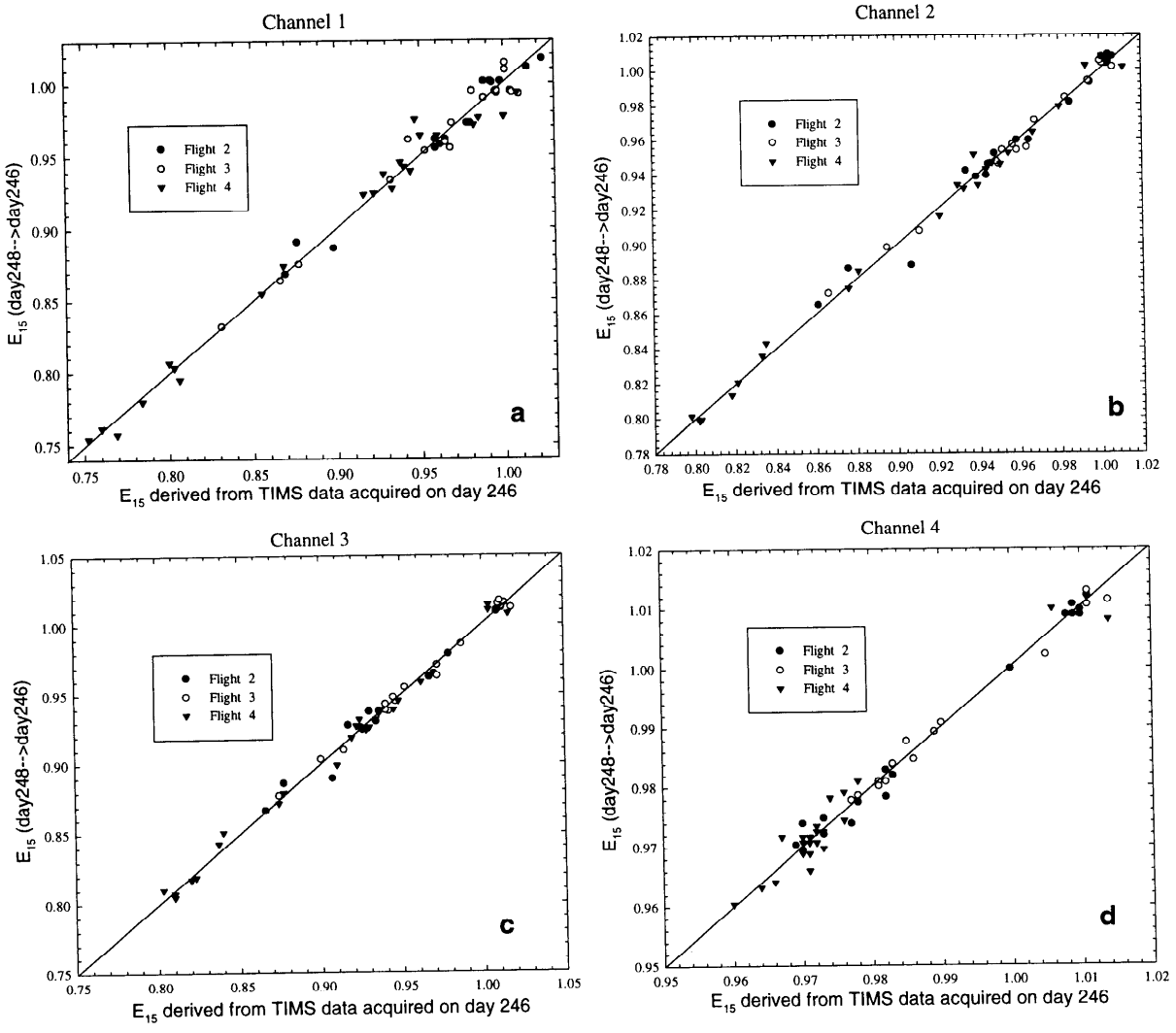

Figure 6. Application of the temporal normalization method to relative emissivities derived from some pixels of the flight lines 2, 3, and 4 of day 248. The ordinate represents the relative emissivities derived from TIMS data of day 248 normalized to atmospheric condition of day 246 using (10), while the abscissa represents the relative emissivities derived from TIMS data of day 246.

identified above in the image of flight 4 and for channels 1-3 of TIMS. The linear relationship is observed as predicted by (8). However, it is more likely that the pixels corresponding to points which are far from the regression lines in Figure 5 do not have the same relative emissivities, as required by (8). This property can be used to check whether the selected pixels do satisfy the condition under which (8) holds. Fourth, after eliminating the points that are far from the regression line, we determine the coefficients of (8), $a(t_2 \rightarrow t_1)$ and $b(t_2 \rightarrow t_1)$, from a linear regression on the remaining points. Finally, with these coefficients we normalize, using (10), the relative emissivities $E^c(t_2)$ calculated from TIMS data of day 248 to the atmospheric condition of day 246 $E^c(t_2 \rightarrow t_1)$ for any pixel in the image. Figure 6 displays this result for some pixels of flights 2, 3, and 4 and for channels 1-4 of TIMS. Since most parts of surfaces are likely to be the same for these two days, most points should be laid on 1:1 line, which is observed with a good accuracy in Figure 6. From those results we can conclude that the temporal atmospheric normalization method makes it possible to monitor the temporal variation of surface spectral properties.

5. Conclusion

The linear relationship between the relative emissivity calculated with uncorrected atmospheric effects and its actual value found by *Li et al.* [1999] has been confirmed with actual TIMS data acquired for the HAPEX-Sahel experiment in 1992. On the basis of this linear relationship property a method called temporal atmospheric normalization has been proposed to monitor the temporal variation of surface spectral properties, correcting for possible temporal variation of atmospheric conditions. One should keep in mind that this method is based on the assumption that no significant spatial variation in atmospheric conditions occurs for a whole image or, at least, that the temporal variation of the atmosphere for the whole image is the same. This assumption may not be valid for a large region and in complicated terrain. In order to check the validity of this assumption it is recommended to find two sets of surface samples having relative emissivities which do not change during the time period of interest. The first set will be used for the linear regression, and the second set will be used to check the assumption of no significant spatial variation in the atmospheric conditions. This method is well suited for EOS ASTER data, and we plan to apply it in the future.

Acknowledgments. We would like to express our gratitude to T.J. Schmugge at USDA Hydrology Laboratory, Beltsville, for providing us with the TIMS data and P. Bessemoulin at CNRM for the radiosonde data. We would like also to think J. Sobrino and an anonymous reviewer for very helpful and stimulating comments that greatly improved the quality of the manuscript. Z.-L.L. wishes to thank M.P. Stoll at LSIIT and the CNRS for allowing him to leave Strasbourg in 1998 and Z. Wan at UCSB for providing him with the financial support during his stay at UCSB. Z.W. is supported by the NASA contract NAS5-31370.

References

Becker, F., and Z.-L. Li, Temperature-independent spectral indices in thermal infrared bands, *Remote Sens. Environ.*, *32*, 17-33, 1990.

Gillespie, A.R., Lithologic mapping of silicate rocks using TIMS, in *The TIMS Data Users' Workshop, JPL Publ., 86-38*, 29-44, 1985.

Gillespie, A.R., S. Rokugawa, S. Hook, T. Matsunaga, and A.B. Kahle, Temperature/emissivity separation algorithm theoretical basis document, version 2.3, Jet Propulsion Lab., Pasadena, Calif., 1996.

Houssa, R., J.-C. Pion, and H. Yesou, Effects of granulometric and mineralogical composition on spectral reflectance of soils in a Sahelian area, *ISPRS J. Photogramm. Remote Sens.*, *51*, 284-298, 1996.

Kahle, A.B., D.P. Madura, and J.M. Soha, Middle infrared multispectral aircraft scanner data: Analysis for geological applications, *Appl. Opt.*, *19*(14), 2279-2290, 1980.

Kahle, A.B., F.D. Palluconi, S. Hook, V. Realmuto, and G. Bothwell, The advanced spaceborne thermal emission and reflectance radiometer (ASTER), *Int. J. Imaging Syst. Technol.*, *3*, 144-156, 1991.

Kealy, P.S., and A.R. Gabell, Estimation of emissivity and temperature using alpha coefficients, in *Proceedings of the Second TIMS Workshop, JPL Publ., 90-55*, 11-15, 1990.

Li, Z.-L., F. Becker, M.P. Stoll, and Z. Wan, Evaluation of six methods for extracting relative emissivity spectra from thermal infrared images, *Remote Sens. Environ.*, *69*, 197-214, 1999.

Kneizys, F.X., et al., The MODTRAN 2/3 report and LOWTRAN 7 model, Ontar Corp., North Andover, Mass., 1996.

Nerry, F., M.P. Stoll, and J.-C. Pion, Infrared spectro-radiometry, In *HAPEX-Sahel Ground Data Version 4, CD-ROM 3*, Cent. Natl. d'Eudes Spatiales, Toulouse, France, 1996.

Palluconi, F., and G.R. Meeks, Thermal infrared multispectral scanner (TIMS): An investigator's guide to TIMS data, *JPL Publ., 85-32*, 1985.

Prince, S.D., et al., Geographical, biological, and remote sensing aspects of the Hydrologic Atmospheric Pilot Experiment in the Sahel (HAPEX-Sahel), *Remote Sens Environ.*, *51*, 215-234, 1995.

Realmuto, V.J., Separating the effects of temperature and emissivity: Emissivity spectrum normalization, *in Proceedings of the Second TIMS Workshop, JPL Publ., 90-55*, 31-35, 1990.

Schmugge, T.J., F. Becker, and Z.-L. Li, Spectral emissivity variations observed in airborne surface temperature measurements, *Remote Sens Environ*, *35*, 95-104, 1991.

Slater, P.N., *Remote sensing optics and optical system*, 575pp, Addison-Wesley, Reading, Mass., 1980.

Steyn-Ross, M.L., D.A. Steyn-Ross, P.J. Smith, and J.D. Shepherd, Water vapor correction method for advanced very high resolution radiometer data, *J. Geophys. Res.*, *98*(C12), 22,817-22,826, 1993.

Steyn-Ross, M.L., D.A. Steyn-Ross, and W.J. Emery, A dynamic water vapor correction method for the retrieval of land surface temperature from AVHRR, *J. Geophys. Res.*, *102*(D16), 19,629-19,643, 1997.

Stoll, M., Restitution de la temperature de surface par teletedection aeroportee dans le cadre de Hapex-Mobilhy. Ph.D Thesis, Paul Sabastier Univ., Toulouse, France, 1993.

Vincent, R.K., and F.J. Thomson, Rock-type discrimination from ratioed infrared scanner images of Pisgah Crater, California, *Science*, *175*, 986-988, 1972.

Wan, Z., and Z.-L. Li, A physics-based algorithm for retrieving land surface emissivity and temperature from EOS/MODIS data, *IEEE Trans. Geosci. Remote Sens.*, *35*(4), 980-996, 1997

Watson, K., Spectral ratio method for measuring emissivity, *Remote Sens Environ.*, *42*, 113-116, 1992.

F. Becker, Z.-L. Li, and M.P. Stoll, Laboratoire des Sciences de l'Image, de l'Informatique et de la Télédétection, 5 Bd. Sebastien Brant, 67400 Illkirch, France. (becker@isu.isunet.edu; Zhao-Liang.Li@mail-grtr.u-strasbg.fr; Marc-Philippe.Stoll@mail-grtr.u-strasbg.fr)

Z. Wan, Institute for Computational Earth System Science, University of California, Santa Barbara, CA93106-3060. (wan@icess.ucsb.edu)

(Received December 21, 1998; revised August 18, 1999; accepted August 26, 1999.)